Post-Stall Lift Enhancement of a Flat Plate Airfoil by Suction

Z. Wang[1] and I. Gursul[2]
Department of Mechanical Engineering, University of Bath, Bath, BA2 7AY, UK

and

J. Wu[3]
China Aerodynamics Research and Development Center, Beichuan, Sichuan, 622750, PR China

The effect of suction on airfoil surface at various locations downstream of the leading-edge of a thin flat-plate airfoil was studied in a wind tunnel at a low Reynolds number. At post-stall angles of attack, substantial lift enhancement and delay of stall can be achieved if a large separation bubble is generated by reattaching the massively separated flow near the trailing-edge. The effects of location and volumetric flow rate of suction were investigated by means of force and velocity measurements. There is an optimal location of suction around x_s/c = 0.4, which generates the maximum lift coefficient for suction coefficients less than 3%. When suction is applied near the leading-edge, it may be easier to reattach the flow for small suction coefficients, but the resulting small separation bubble causes smaller lift increase. The size of the separation bubble is important, and small bubbles can even cause smaller lift enhancement than the separated flows due to the suction further downstream.

Nomenclature

b	=	span
c	=	chord length
C_Q	=	suction coefficient ($Q/U_\infty S$)
C_L	=	lift coefficient
q	=	free-stream dynamic pressure
Q	=	suction volumetric flow rate
Re	=	Reynolds number
S	=	airfoil surface area
t	=	airfoil thickness
U_∞	=	free-stream velocity
x_s	=	chordwise location of suction
α	=	angle of attack
ν	=	fluid kinematic viscosity
ρ	=	air density
ω	=	spanwise vorticity

1. Introduction

This research falls into the category of active flow control of massively separated flows over sharp-edged airfoils and thin airfoils. Sharp edges are common for many fighter aircraft. Thin airfoils are also commonly used in low Reynolds number aerodynamics [1]. Extremely thin cross-sections are typical in biological flows of insects [2]. Flow separation is unavoidable at the leading-edge of thin airfoils even at low-to-moderate angels of attack. Of course, for rounded leading-edge airfoils, flow separation at the leading-edge is also unavoidable at high angles of attack. This research focusses on the cases where the flow separates at the leading-edge and the delay of flow

[1] Lecturer, Department of Mechanical Engineering, Member AIAA.
[2] Professor, Department of Mechanical Engineering, Associate Fellow AIAA.
[3] Senior Engineer, China Aerodynamics Research and Development Center, Beichuan, Sichuan, 622750, PR China.

separation is difficult due to the sharp-edges or thin cross-sections. Therefore, classical *boundary-layer separation control* will not be attempted. This alternative is well understood, and the most effective techniques rely on unsteady excitation/forcing of weakly separated boundary-layer flow [3]. However, it is not as effective in the case of sharp-edges or thin cross-sections as the separated flow cannot reattach. If the flow is forced periodically at the leading-edge, even though completely reattached flow is not established, discrete leading-edge vortices still increase the lift as they are convected downstream. Examples of this type of control for massively separated flows include unsteady blowing-suction [4] and oscillating mini-flap [5] near the leading-edge, and small-amplitude airfoil oscillations [6]. Lack of complete reattachment can be reversed if there is sufficient wing sweep owing to the spanwise removal of vorticity [7].

There have been other approaches to obtain high lift in massively separated flows. *Leading-edge vortex lift* is known to be important in achieving high lift coefficients for insect flight [8]. High lift using a vortex over an airfoil has been modelled by Saffman and Sheffield [9]. Unfortunately, vortex is not stable and prone to shedding in real flows. Two concepts were included in later studies to stabilize the vortex [10]. First, the use of sink in the vortex core (blowing or suction in the spanwise direction in real flows) revealed that vortex is still unstable even for high blowing/suction rates. (Of course, the unstable vortices in the two-dimensional case are different than the stable vortices over highly swept wings or rotating wings). Second, the addition of leading-edge and trailing-edge fences was considered [10]. However, reattachment to the trailing- edge fences was not observed in the wind tunnel experiments.

Our approach will be to achieve a stable separation bubble and complete flow reattachment by means of suction downstream of the leading-edge region. The studies of boundary layer control using suction can be traced back to much earlier work by Prandtl [11]. Previous studies confirmed that flow control with suction could be used to delay flow separation for airfoils and wings [12]. There is recent evidence that suction might be more effective than blowing for the flow control on a thick airfoil [13]. In the case of highly three-dimensional separated flows over slender delta wings, suction at the sharp leading-edge can manipulate the structure of the leading-edge vortex and breakdown [14]. In this study we do not try to delay flow separation as it is unavoidable at the leading-edge of a flat plate airfoil. We rather apply suction downstream on the airfoil surface, with the purpose of forming a large separation bubble. It is known that formation of a large separation bubble by reattaching a formerly separated flow can lead to substantial improvement in low Reynolds number aerodynamics [15]. This paper reports an experimental study of the effects of suction on the aerodynamics of a flat plate airfoil, with emphasis on increasing lift and delaying stall of the airfoil. Both force measurements and flow field measurements using Particle Image Velocimetry (PIV) were conducted in a wind tunnel. The effects of location and volumetric flow rate of suction were investigated.

2. Experimental Methods

A. Experimental Setup

The experiments were carried out in a low-speed, closed-loop open-jet wind tunnel with a circular working section of 760 mm in diameter, located in the Department of Mechanical Engineering, at the University of Bath. The tunnel has a maximum speed of 30 m/s and a freestream turbulence level of 0.1%. The thin flat plate airfoil, which was made from aluminium sheet, has a chord length of c = 200 mm, a span of b = 400 mm, a thickness of t = 10 mm, and rounded (semi-circle) leading and trailing edges. The hollow airfoil had five spanwise slots of 1 mm width at x_s/c = 0.05, 0.2, 0.4, 0.6 and 0.8. Two circle end-plates were used to prevent airflow leakage from the bottom surface of the airfoil to the upper surface and maintain a nominally two-dimensional airfoil flow. A schematic of the experimental setup is shown in Figure 1. A Numatic WVD900-2 vacuum cleaner was used to produce suction. Various volumetric flow rates of suction were tested. The volumetric flow rate of suction, adjusted by using a regulator valve, was directly measured using a Trogflux FVA Rotameter. It was previously found that lift enhancement by suction downstream of the natural separation line depends only on volumetric flow coefficient C_Q rather than momentum coefficient C_μ [13]. This is the reason that volumetric flow coefficient was used in this study to characterize the effect of suction. Experiments were conducted at a constant free-stream velocity of U_∞ = 5 m/s, giving a Reynolds number ($Re = U_\infty c/\nu$, where U_∞ is the free-stream velocity and ν is the fluid kinematic viscosity) of $Re = 6.7\times10^4$.

B. Force Measurements

The assembly of the airfoil and end plates was mounted vertically to the tunnel ceiling support via a two-component aluminium binocular strain gauge force balance, which was used to measure the axial force and normal

force on the airfoil. Signals from the force balance were simultaneously digitized using a 12 bit A/D board and a personal computer at a sampling frequency of 1 kHz per channel. The duration of each record was about 10 seconds. This has been verified to be sufficiently long for the root mean square (rms) value of the measured signals to reach a steady value (variation less than 1.0%). The measured axial and normal forces were used to calculate the lift force of the airfoil, which was then normalized by qS, where $q = \frac{1}{2}\rho U_\infty^2$ is the free-stream dynamic pressure, and S is the planform surface area, to calculate the lift coefficient. The measurement uncertainty for the lift coefficient is estimated to be 4%.

C. PIV Measurements

A TSI 2D-PIV system was used to measure the velocity field over the airfoil. The airfoil surface was painted black to minimize the reflection noise. The flow was seeded with oil droplets produced by a TSI model 9307-6 multi-jet atomizer. The atomizer worked best using olive oil and the mean size of the droplets was 1 μm. The PIV camera was placed underneath the tunnel working section to measure the velocity field in a streamwise plane. Illumination was provided by the laser sheets (with a thickness of 2 mm) generated by a combination of cylindrical and spherical lenses from a pair of pulsed 50 mJ Nd:YAG lasers at the mid-span of the airfoil. Because of the relatively large chord length, the flow field was imaged in three separate regions. The digital particle images from the PIV measurements were taken using an 8- bit CCD camera with a resolution of 1600 by 1192 pixels. The commercial software package Insight 3G and a Hart cross-correlation algorithm were used to analyse the images. For the image processing, an interrogation window size of 32×32 pixels was used, and thus producing velocity vectors for further processing. The effective grid size was around 2.25 mm. The estimated uncertainty for velocity measurements is 2% of the freestream velocity U_∞. For each case, sequences of 200 instantaneous frames were taken, and the time-averaged velocity and vorticity fields were calculated.

3. Results and Discussion

A. Effect of Angle of Attack

Figure 2 presents the variation of the time-averaged lift coefficient C_L with incidence for the flat-plate airfoil without and with suction of different volumetric coefficients at $x_s/c = 0.4$. It can be observed that, without suction flow control, C_L increases with incidence and reaches the maximum value of $C_{L,max} \approx 0.87$ at $\alpha = 9^\circ$. With suction at $x_s/c = 0.4$, the effect is negligible for pre-stall angles of attack. However, at post-stall angles of attack, the lift enhancement can be substantial. The almost linear part of the lift coefficient curve can be extended to higher angles of attack with increasing suction coefficient. For the maximum suction coefficient shown in Figure 2, the stall angle is delayed to 14 degrees. Around this angle of attack the effect of suction coefficient (dC_L/dC_Q) appears to be large. With increasing angle of attack, particularly for $\alpha > 20$ degrees, suction loses its effectiveness. In summary, suction appears to be effective at post-stall angles of attack, but just above the stall angle.

Corresponding streamline patterns and vorticity fields of the time-averaged flow are shown in Figures 3 and 4 for no suction (left column) and with suction (right column) at different angles of attack. For these figures, the suction coefficient was kept at $C_Q = 0.0292$ at $x_s/c = 0.4$, which was also the largest value used in Figure 2. It is seen that, for the pre-stall angles of attack $\alpha = 5^\circ$ and $\alpha = 8^\circ$, there is a laminar separation bubble for the no suction case, and the time-averaged reattachment location moves downstream with increasing angle of attack. With suction at $x_s/c = 0.4$, the size of the separation bubble becomes smaller for $\alpha = 8^\circ$, however the effect on lift is apparently small (see Figure 2). For just above the stall angle, the reattachment line appears to have just moved off the surface of the airfoil for $\alpha = 10^\circ$ with no suction. However, with suction, the reattachment moves upstream near the location of suction. At this angle of attack, there is already a significant increase in lift with suction. It appears from Figure 2 that this lift enhancement could have been obtained for a smaller suction coefficient. The effect of suction coefficient will be discussed later on.

At a larger angle of attack of $\alpha = 12^\circ$, with no suction, there is a large recirculation region in the time-averaged flow, indicating the completely separated flow without reattachment. With suction, the reattachment location moves onto the airfoil surface and closer to the location of suction, similar to the previous angle of attack. However, the height of the bubble is larger, resulting in a larger lift coefficient. Even at $\alpha = 15^\circ$, suction is capable of bringing the reattachment location onto the airfoil surface and near the trailing-edge, resulting in a larger bubble height and enhanced lift. At larger angles of attack of $\alpha = 17^\circ$ and $\alpha = 19^\circ$, the size of the massively separated flow region increases with no suction, and the reattachment is not observed on the airfoil with suction, resulting in a decrease in the lift coefficient.

Figure 4 shows that the spanwise vorticity magnitude diffuses quickly if there is no reattachment. This is due to the transition to turbulence and increasing three-dimensionality of the separated shear layer, which appears to diffuse when time-averaged. Nevertheless, the effect of suction is visible when the direction of the separated shear layer at the leading-edge is observed.

B. Effect of Suction Coefficient

Figure 2 suggests that the effect of suction coefficient can be substantial, depending on the angle of attack. In order to investigate this effect in more detail, we carried out PIV measurements for α = 15º and α = 19º, corresponding to the data shown in Figure 2 for the suction location of x_s/c = 0.4. These are shown in Figures 5 and 6. In these figures, the streamline patterns and spanwise vorticity magnitude of the time-averaged flow are shown for varying suction coefficients. Figure 5 reveals that, complete flow reattachment is only possible for the largest suction coefficient for α = 15º. It is interesting that the lift enhancement due to the suction is still significant for smaller suction coefficients even though there is no reattachment. For these cases, the decrease in the size of the separation region is apparent. Also, the distortion in the internal structure of the recirculation region due to the suction becomes more noticeable with increasing suction coefficient.

At the larger angle of attack of α = 19º, there is no reattachment for any suction coefficient as seen in Figure 6. Overall, at this angle of attack, suction is less effective compared to α = 15º. Again, there is a slight decrease in the size of the separation zone, and the center of the region of closed streamlines moves closer to the airfoil surface with suction. The effect of the sink at x_s/c = 0.4 is visible. The fluid close to the airfoil surface moves upstream and is withdrawn into the airfoil at x/c = 0.4. The fluid layer just above this region is still part of the recirculation region.

As the effect of suction on the recirculation zone is apparent (especially with increasing suction coefficient), we considered whether this could be exploited by moving the location of suction upstream, closer to the origin of the separated shear layer. For the same angle of attack of α = 19º and the same suction coefficients used at x_s/c = 0.4 (shown in Figure 6), the velocity measurements were repeated for an upstream location of suction at x_s/c = 0.2. Figure 7 shows the streamline patterns and the magnitude of the spanwise vorticity. Only at the largest suction coefficient, there is an indication that suction becomes more effective, achieving reattachment near the trailing-edge. For smaller suction coefficients, there is negligible difference in the flow fields. Further force measurements, which will be discussed below, confirm that the lift force does not change much for these cases. It is clear that both the location and magnitude of suction may be important in some cases, whereas the effect of suction coefficient is small in some other cases. Detailed investigation of the effect of the location of suction is discussed further below.

C. Effect of Suction Location

Figure 8 shows the variation of the lift coefficient as a function of angle of attack for different locations of suction. Lift enhancement at post-stall angles of attack is common to all suction locations. The maximum lift coefficient that can be achieved appears to increase as the location of suction is moved downstream until x_s/c = 0.4. When suction was applied at x_s/c = 0.4, $C_{L,max} \approx 1.44$ was observed at α = 14º for $C_{Q,max}$ = 0.0292. The maximum lift coefficient starts to decrease at x_s/c = 0.6 and x_s/c = 0.8. Hence it appears that, in terms of the maximum lift coefficient that can be achieved, there is an optimal location of suction, which is around x_s/c = 0.4. Also, for the same values of C_Q, the effectiveness appears to decrease when the suction is applied further downstream of x_s/c = 0.4. The maximum delay of the stall, however, is observed for x_s/c = 0.2, and is around $\Delta\alpha \approx 9°$.

The effect of suction coefficient is qualitatively similar for all suction locations, except for the most upstream location of x_s/c = 0.05 for which the effect of suction coefficient is small in the region of maximum lift coefficient. This can be seen more clearly in Figure 9 where the variation of the lift coefficient at α = 15º as a function of suction coefficient is shown for the locations of suction x_s/c = 0.05, 0.2 and 0.4. Early saturation of lift enhancement at small suction coefficients for x_s/c = 0.05 is apparent. There is a similar plateau for x_s/c = 0.2 at higher suction coefficients. It is likely that there will be a similar saturation for x_s/c = 0.4 at very high suction coefficients not tested in these experiments. It is concluded from Figure 9 that, at relatively smaller values of C_Q , the suction flow control technique appears to be more effective when it is applied close to the leading edge of the airfoil, for example at x_s/c =0.05. For the x_s/c =0.05 and x_s/c = 0.2 cases, however, the increase in C_L becomes saturated at around $C_Q \approx$ 0.006 and $C_Q \approx 0.017$, respectively. Figure 9 also implies that the optimal location of suction varies with the range of suction coefficient, however the maximum lift coefficient that can be achieved is around x_s/c = 0.4 for the flat-plate airfoil (see also Figure 8) in the range of $C_Q < 3\%$.

Returning to the saturation effect for the most upstream location of suction x_s/c = 0.05 discussed above, velocity measurements for C_Q = 0.0125 are shown in Figure 10. This value of the suction coefficient is in the saturation region as seen in Figure 9. The streamline patterns suggest that there is a small laminar separation bubble forming

near the leading-edge and the reattachment occurs further downstream of the location of suction. It is interesting that the flow separation cannot be delayed, but the suction promotes the reattachment further downstream. No further velocity measurements were taken for larger suction coefficients in the saturation region. However, we believe that the flow pattern will not change much with increasing suction beyond $C_Q = 0.0125$ shown in Figure 10.

For the same value of suction coefficient $C_Q = 0.0125$, the effect of the location of suction on the flow pattern is shown in Figure 11 for $x_s/c = 0.2$, 0.4, 0.6, and 0.8. Together with $x_s/c = 0.05$ shown in Figure 10, this figure reveals that the reattachment is not possible with the suction location moving downstream for $C_Q = 0.0125$. For this suction coefficient, the suction location of $x_s/c = 0.2$ provides slightly larger lift coefficient than the other locations (see Figure 9). This is perhaps due to the very small separation bubble for $x_s/c = 0.05$. It is interesting that the reattached flow for $x_s/c = 0.05$ has slightly smaller lift coefficient than the separated flow for $x_s/c = 0.2$.

Figure 12 shows the streamline patterns and spanwise vorticity fields when the suction coefficient is increased to $C_Q = 0.0292$ for $x_s/c = 0.2$, 0.4, 0.6, and 0.8. Reattachment downstream of the location of suction for $x_s/c = 0.2$ and 0.4 is visible. The maximum lift coefficient is achieved for $x_s/c = 0.4$ in this case. It is clear that the reattachment on the airfoil surface and the resulting large separation bubble are essential for high lift enhancement. Within the potential flow theory, this lift enhancement effect can be attributed to the camber effect of the large separation bubble.

4. Conclusions

Flow control of massively separated flows over an airfoil was investigated experimentally. The effects of suction on the aerodynamics of a thin flat plate airfoil have been studied in a wind tunnel at a Reynolds number of $Re = 6.7 \times 10^4$. The approach is aimed at generating separation bubbles by reattaching a formerly separated flow by means of suction on the airfoil surface and further downstream of the leading-edge. In the absence of suction, flow separation is unavoidable at the leading-edge of the thin flat-plate airfoil. The effects of location and volumetric flow rate of suction were investigated by means of force and velocity measurements.

Force measurements revealed that the effect of suction is negligible at pre-stall angles of attack, even though, with no suction, there is a laminar separation bubble, which becomes smaller when suction is applied. The lift enhancement can be substantial at post-stall angles of attack, with a maximum of 65% increase in the maximum lift coefficient and a maximum delay of $\Delta\alpha \approx 9°$ for suction coefficients less than 3%. The best performance is observed when the reattachment is achieved on the airfoil surface and close to the trailing-edge, resulting in a large separation bubble. In the cases when reattachment is not achieved, there is smaller lift enhancement. It appears that there is an optimal location of suction around $x_s/c = 0.4$, which generates the maximum lift coefficient for the range of $C_Q <$ 3%. When suction was applied close to the leading-edge, such as $x_s/c = 0.05$, the separation could not be delayed, but reattachment further downstream was promoted, resulting in a small separation bubble. In this case, lift enhancement saturates at small suction coefficients, and can be even slightly smaller than the lift enhancement of a separated flow due to the suction further downstream on the airfoil. Reattachment and resulting lift saturation occur at increasing suction coefficients as the location of suction is moved downstream. Optimal lift enhancement due to the large separation bubble can be attributed to the camber effect within the potential flow theory.

References

[1]Pelletier, A. and Mueller, T.J., "Low Reynolds Number Aerodynamics of Low Aspect Ratio, Thin/Flat/Cambered-Plate Wings", *Journal of Aircraft,* vol. 37, no. 5, 2000, pp. 825-832.

[2]Shyy, W., Berg, M. and Ljungqvist, D., "Flapping and Flexible Wings for Biological and Micro Air Vehicles", *Progress in Aerospace Sciences*, vol. 35, no. 5, 1999, pp. 455-505.

[3]Seifert, A., Bachar, T., Koss, D., Shepshelovich, M. and Wygnanski, I., "Oscillatory Blowing: a Tool to Delay Boundary-Layer Separation", *AIAA Journal*, vol. 31, 1993, pp. 2052-2060.

[4]Wu, J-Z., Lu, X-Y., Denny, A.G., Fan, M. and Wu, J-M., "Post-Stall Flow Control on an Airfoil by Local Unsteady Forcing", *Journal of Fluid Mechanics,* vol. 371, 1998, pp. 21-58.

[5]Miranda, S., Vlachos, P.P., Telionis, D.P. and Zeiger, M.D., "Flow Control of a Sharp-Edged Airfoil", *AIAA Journal,* vol. 43, 2005, pp. 716-726.

[6]Cleaver, D.J., Wang, Z. and Gursul, I., "Investigation of High-Lift Mechanisms for a Flat-Plate Airfoil Undergoing Small-Amplitude Plunging Oscillations", *AIAA Journal,* vol. 51, No. 4, 2013, pp. 968-980.

[7]Vardaki, E., Wang, Z. and Gursul, I., "Flow Reattachment and Vortex Re-formation on Oscillating Low-Aspect Ratio Wings", *AIAA Journal,* vol. 46, 2008, pp. 1453-1462.

[8]Ellington, C., "The Aerodynamics of Hovering Insect Flight. IV. Aerodynamic Mechanisms", *Philos. Trans. R. Soc. London*., Ser. B, 305, 1984, pp. 79-113.

[9]Saffman, P. and Sheffield, J., "Flow over a Wing with an Attached Free Vortex", *Stud. Appl. Math.*, 57, 1977, pp. 107-117.

[10]Rossow, V., "Lift Enhancement by an Externally Trapped Vortex", *Journal of Aircraft,* vol. 15, no. 9, 1978, pp. 618-625.

[11]Schlichting, H., *Boundary-Layer Theory*, McGraw-Hill, Seventh Edition, 1979.
[12]Lachmann, G.V., *Boundary Layer and Flow Control*, Edited, Pergamon Press, London, 1961.
[13]Chen, C., Seele, R. and Wygnanski, I., "Flow Control on a Thick Airfoil using Suction Compared to Blowing", *AIAA Journal,* vol. 51, no. 6, 2013, pp. 1462-1472.
[14]McCormick, S. and Gursul, I., "Effect of Shear-Layer Control on Leading-Edge Vortices", *Journal of Aircraft,* vol. 33, no. 6, 1996, pp. 1087-1093.
[15]Yang, S.L. and Spedding, G.R., "Separation Control by External Acoustic Excitation at Low Reynolds Numbers", *AIAA Journal,* vol. 51, no. 6, 2013, pp. 1506-1515.

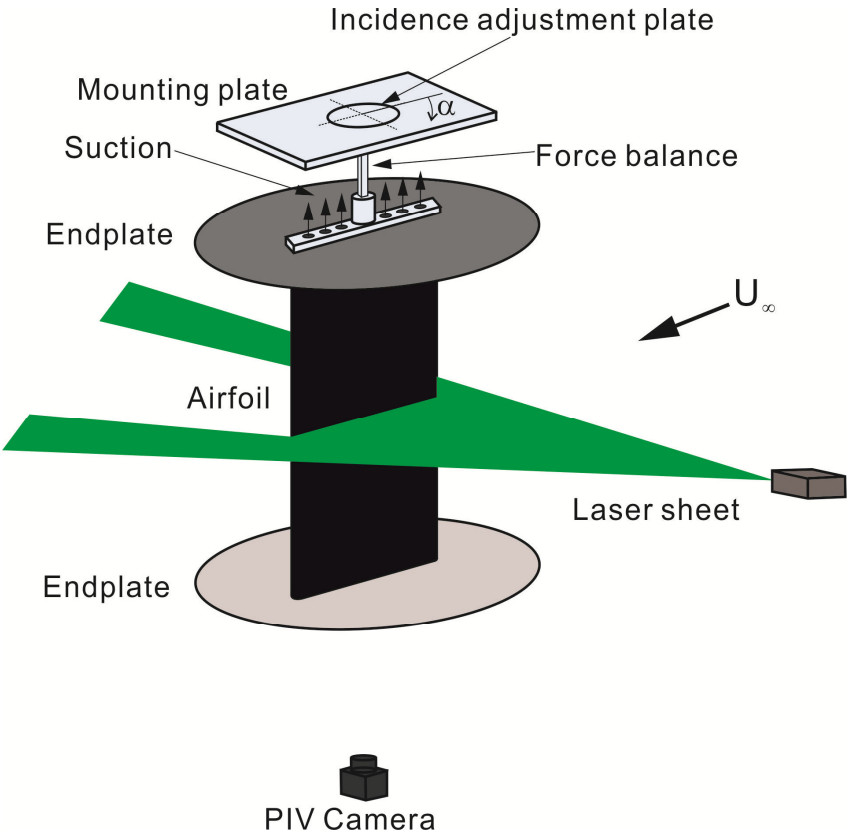

Figure 1. Experimental setup

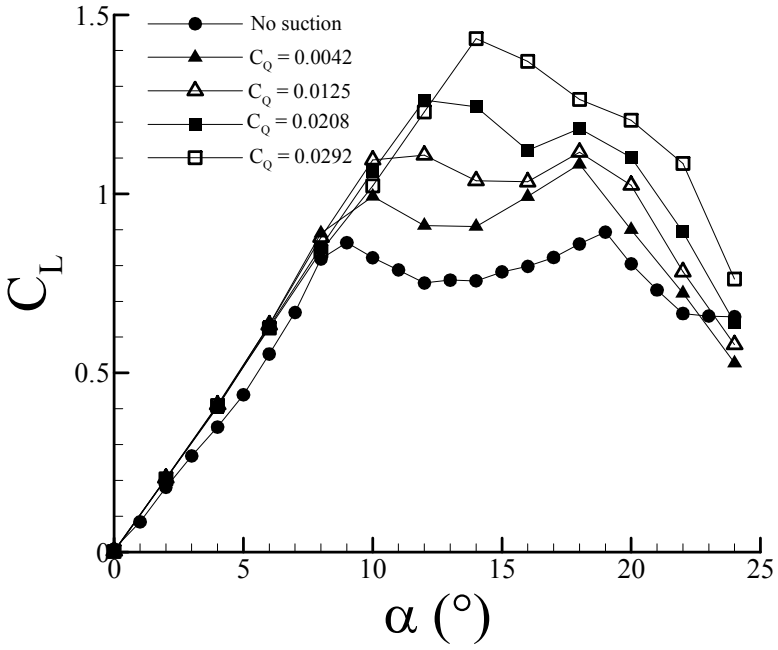

Figure 2. Variation of time-averaged lift coefficient with incidence for the flat-plate airfoil without and with suction of different volumetric coefficients at x_s/c = 0.4.

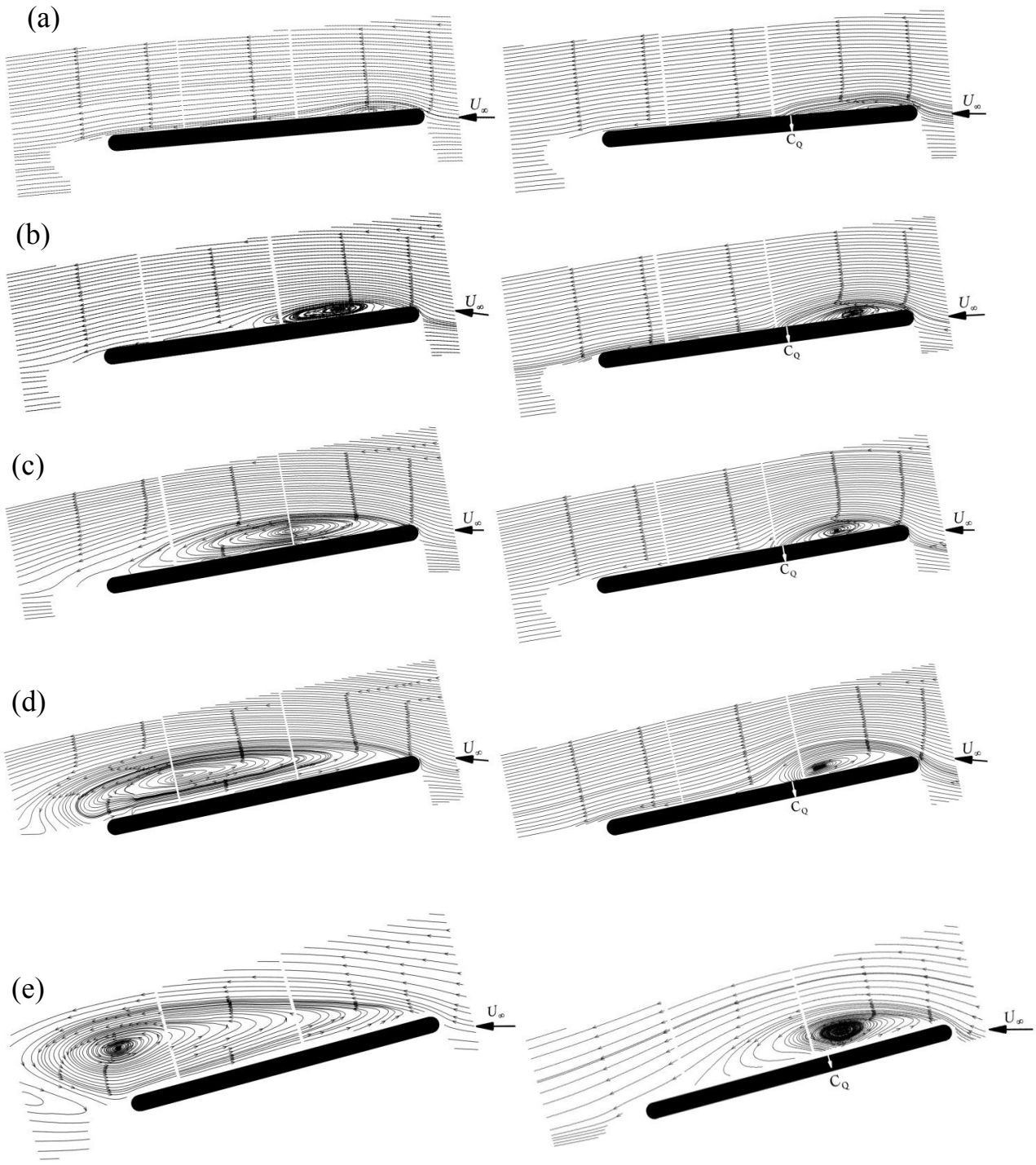

Figure 3. Streamline pattern in the mid-span plane over the flat-plate airfoil without suction (left column) and with suction of C_Q = 0.0292 at x_s/c=0.4 (right column) at (a) α = 5º; (b) α = 8º; (c) α = 10º; (d) α = 12º; (e) α = 15º; (f) α = 17º; (g) α = 19º.

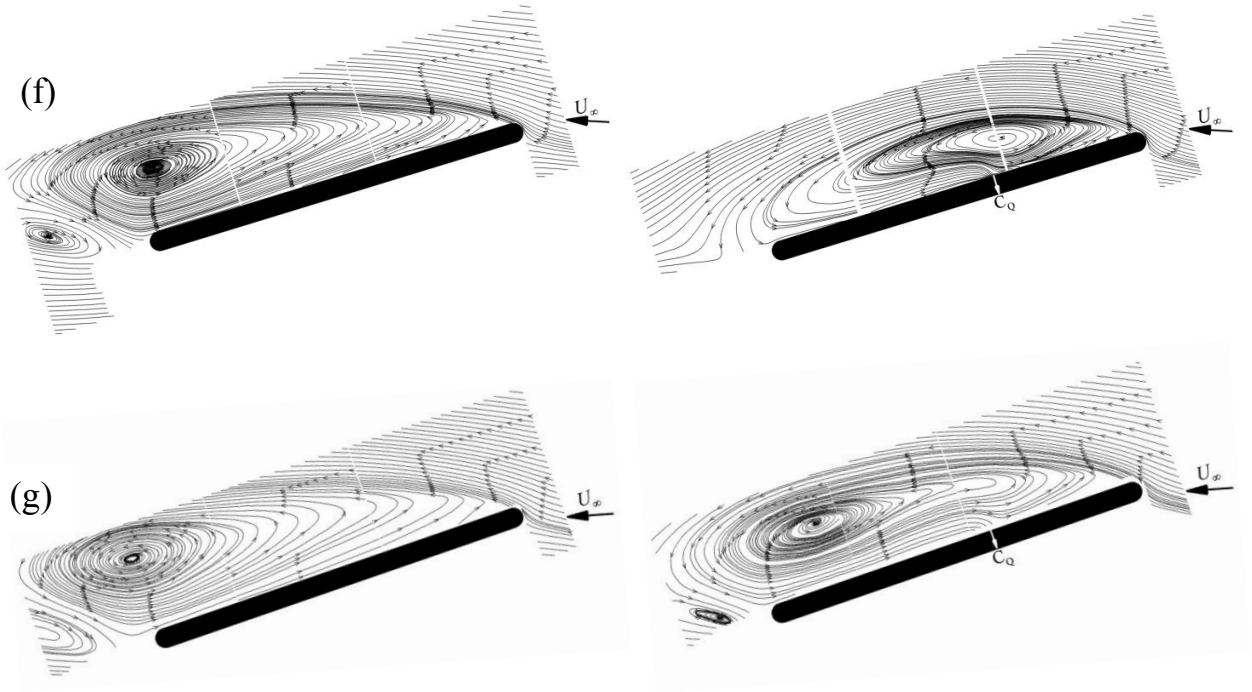

Figure 3 (Continued).

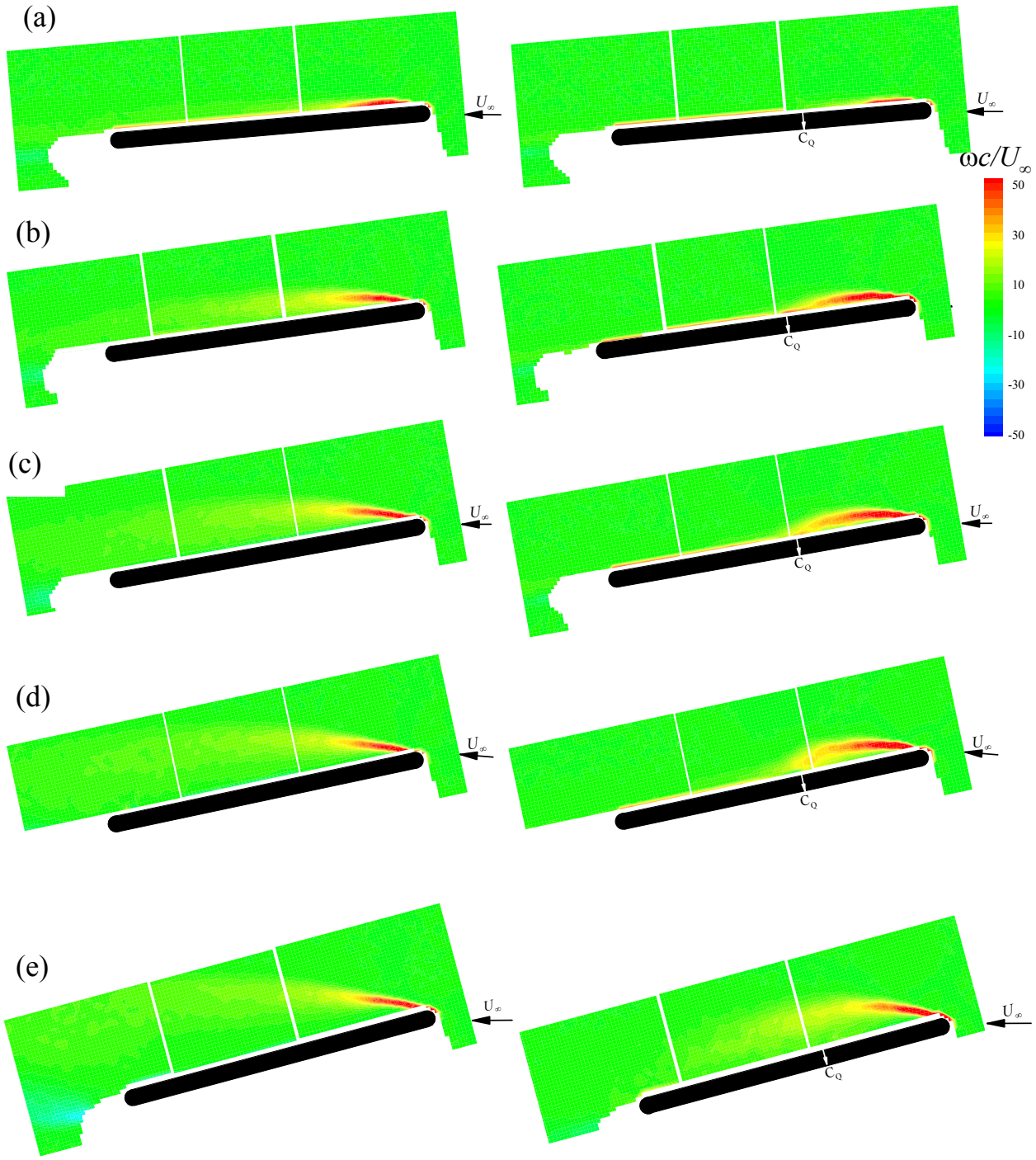

Figure 4. Non-dimensional spanwise vorticity measured in a streamwise plane at midspan of the flat-plate airfoil without suction (left column) and with suction of C_Q = 0.0292 at x_s/c=0.4 (right column) at (a) α = 5°; (b) α = 8°; (c) α = 10°; (d) α = 12°; (e) α = 15°; (f) α = 17°; (g) α = 19°.

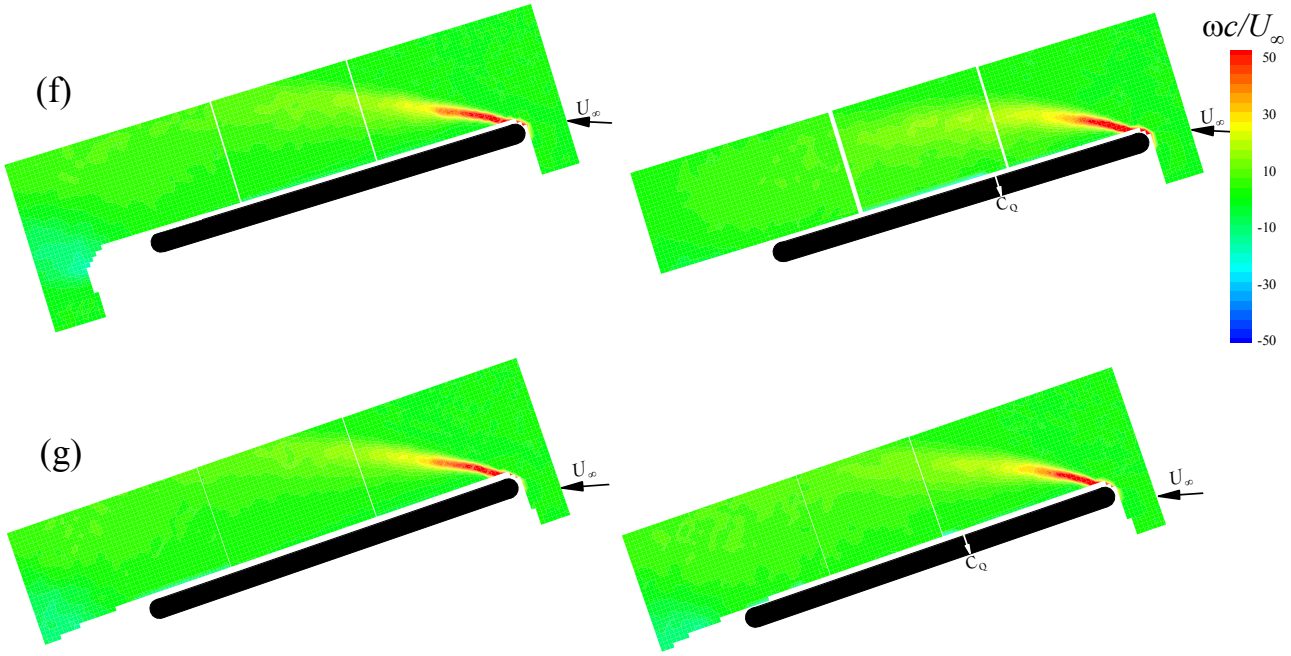

Figure 4 (Continued).

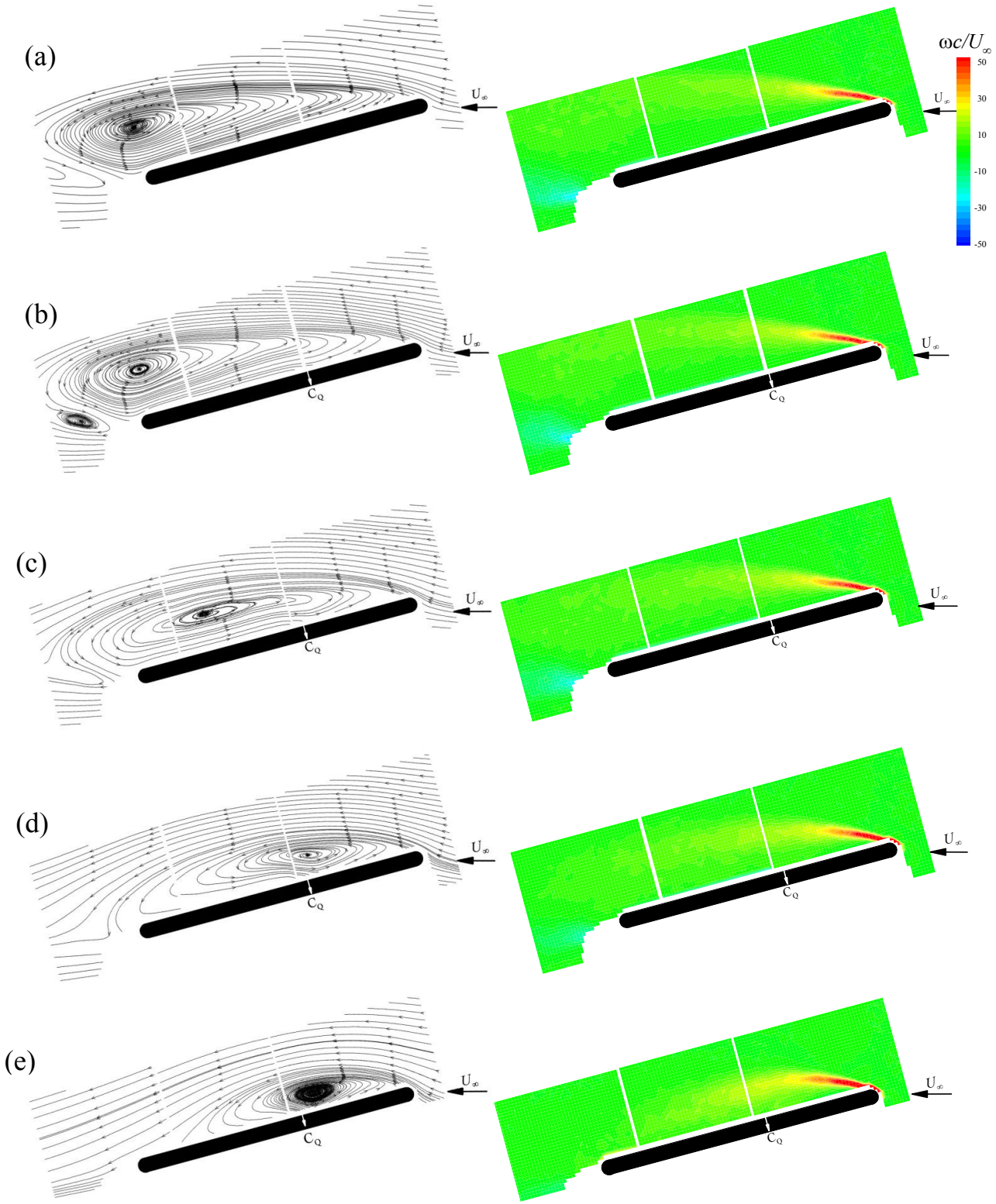

Figure 5. Streamline pattern (left column) and non-dimensional spanwise vorticity (right column) measured in a streamwise plane at midspan of the flat-plate airfoil at $\alpha = 15^o$ with suction at x_s/c=0.4. (a) No suction; (b) $C_Q = 0.0042$; (c) $C_Q = 0.0125$; (d) $C_Q = 0.0208$; (e) $C_Q = 0.0292$.

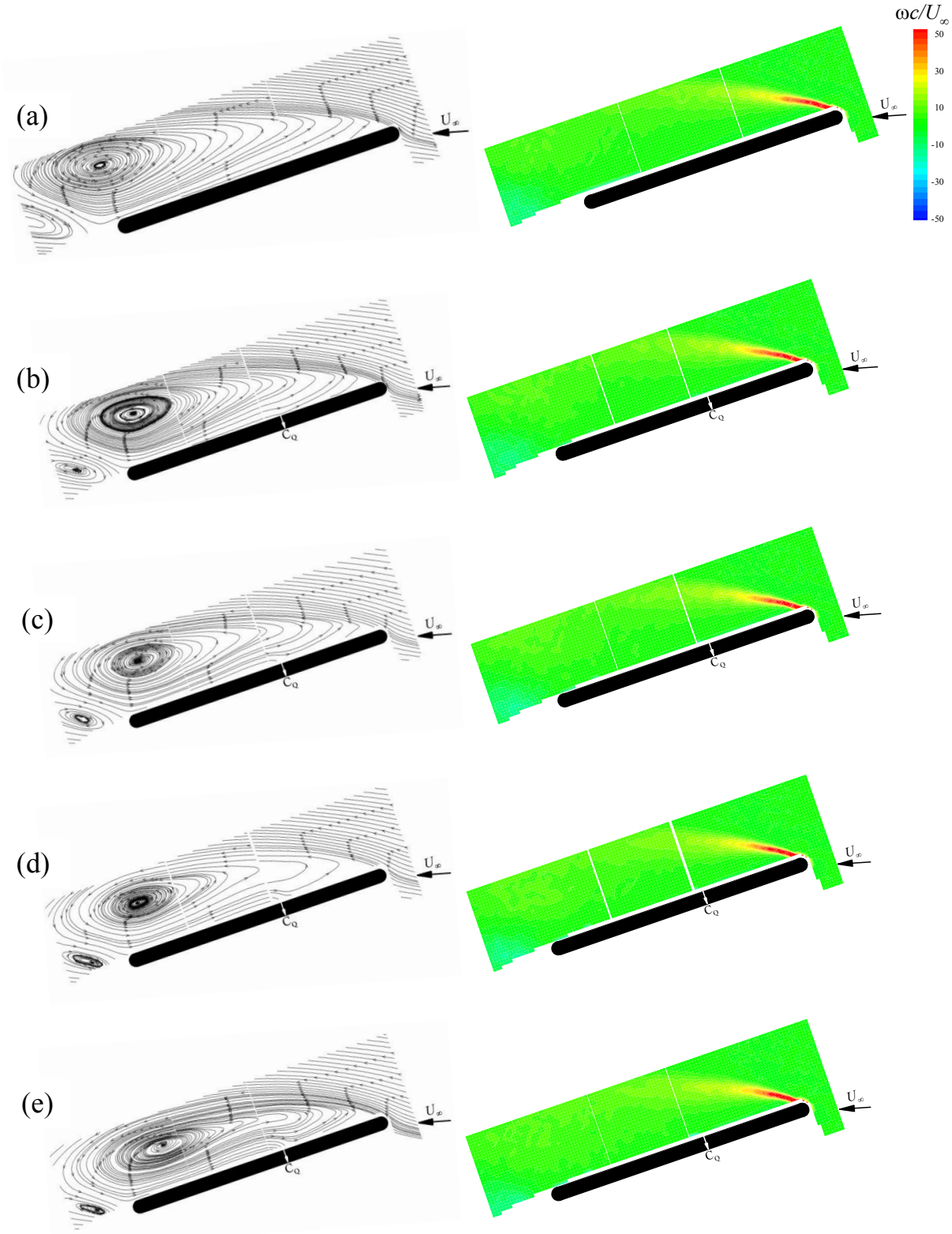

Figure 6. Streamline pattern (left column) and non-dimensional spanwise vorticity (right column) measured in a streamwise plane at midspan of the flat plate airfoil at $\alpha = 19^{o}$ with suction at x_s/c=0.4. (a) No suction; (b) C_Q = 0.0042; (c) C_Q = 0.0125; (d) C_Q = 0.0208; (e) C_Q = 0.0292.

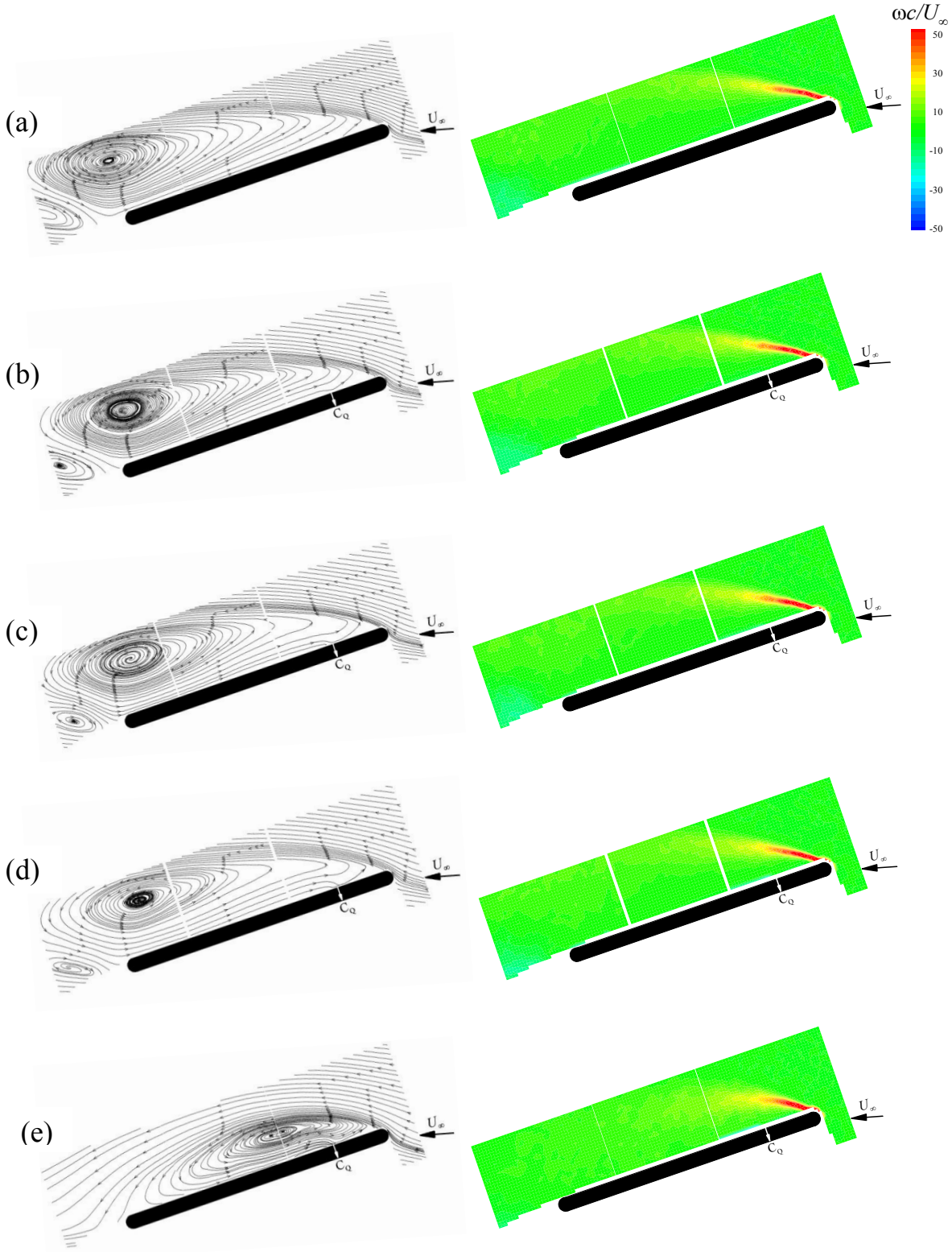

Figure 7. Streamline pattern (left column) and non-dimensional spanwise vorticity (right column) measured in a streamwise plane at midspan of the flat-plate airfoil at α = 19° with suction at x_s/c=0.2. (a) No suction; (b) C_Q = 0.0042; (c) C_Q = 0.0125; (d) C_Q = 0.0208; (e) C_Q = 0.0292.

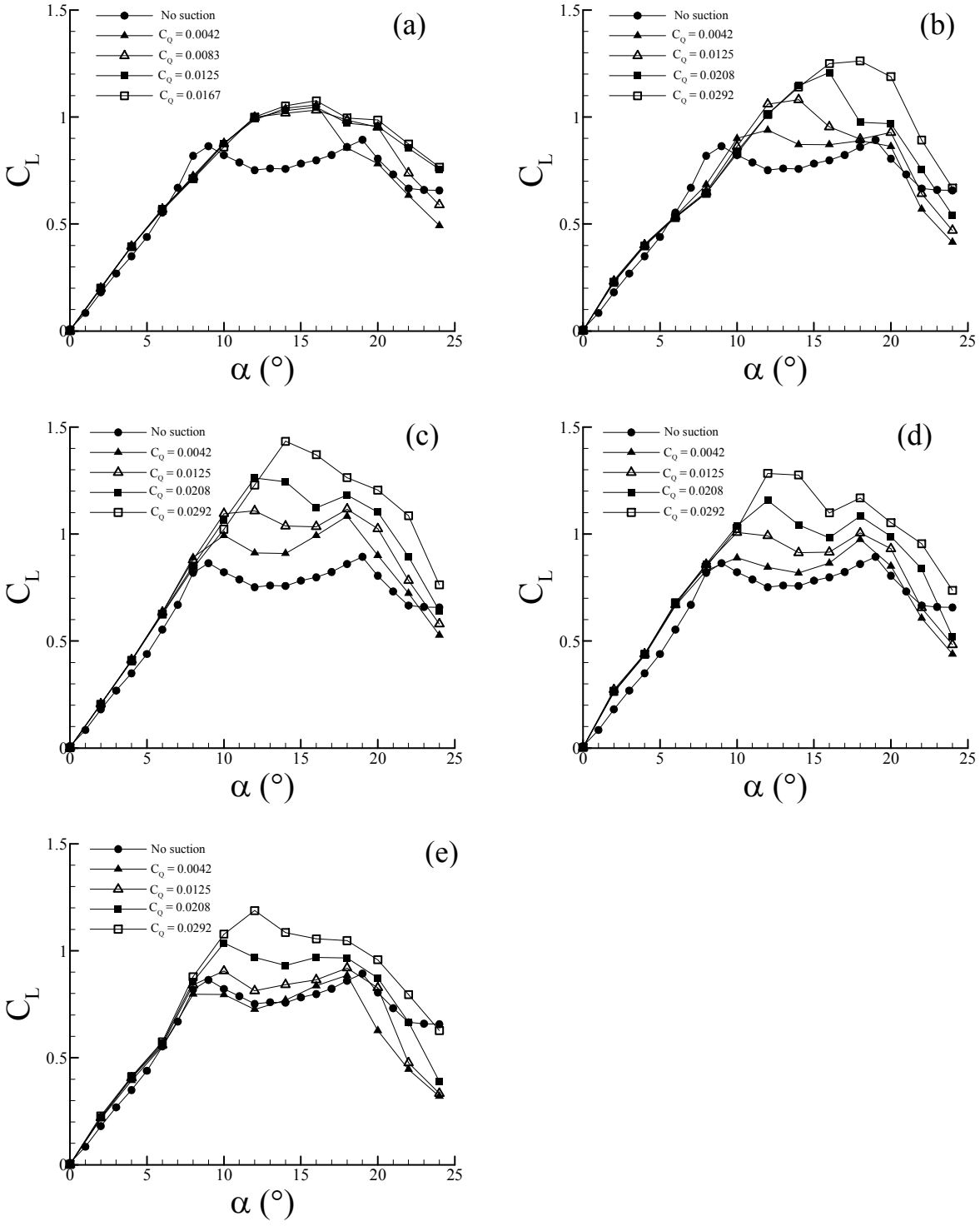

Figure 8. Variation of time-averaged lift coefficient with incidence for the flat-plate airfoil without and with suction of different volumetric coefficients at (a) x_s/c = 0.05, (b) x_s/c = 0.2, (c) x_s/c = 0.4, (d) x_s/c = 0.6, (e) x_s/c = 0.8.

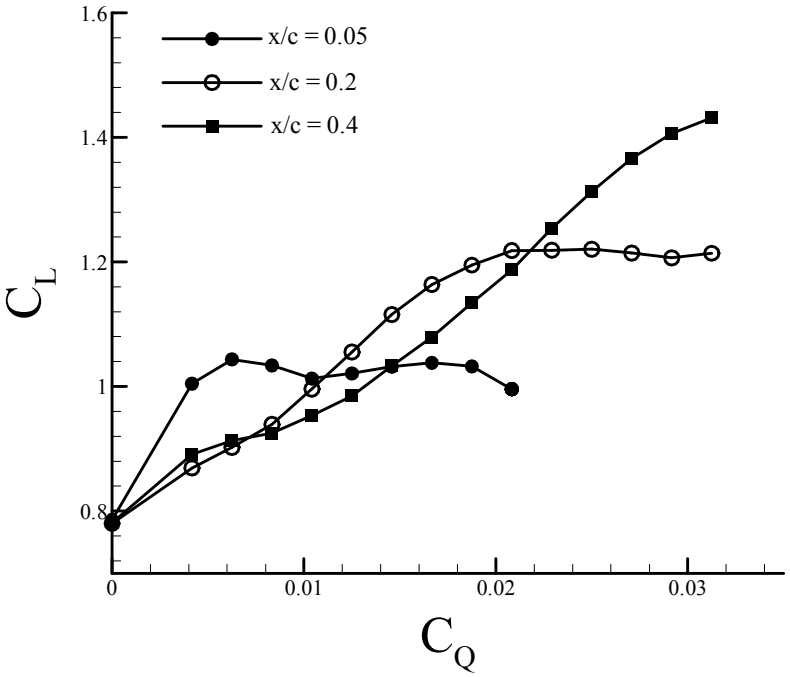

Figure 9. Variation of time-averaged lift coefficient with suction coefficient for the flat-plate airfoil with suction at various chordwise locations, $\alpha = 15^{o}$.

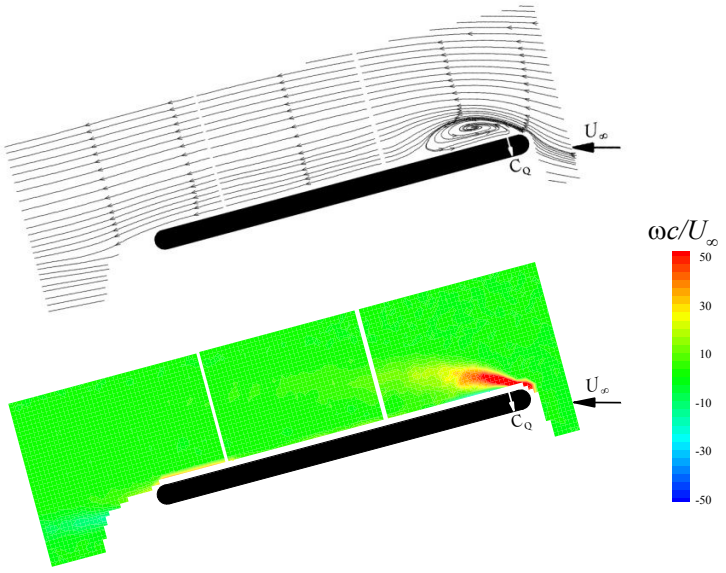

Figure 10. Streamline pattern and non-dimensional spanwise vorticity measured in a streamwise plane at midspan of the flat-plate airfoil at $\alpha = 15^{o}$ with suction of $C_Q = 0.0125$ at x_s/c=0.05.

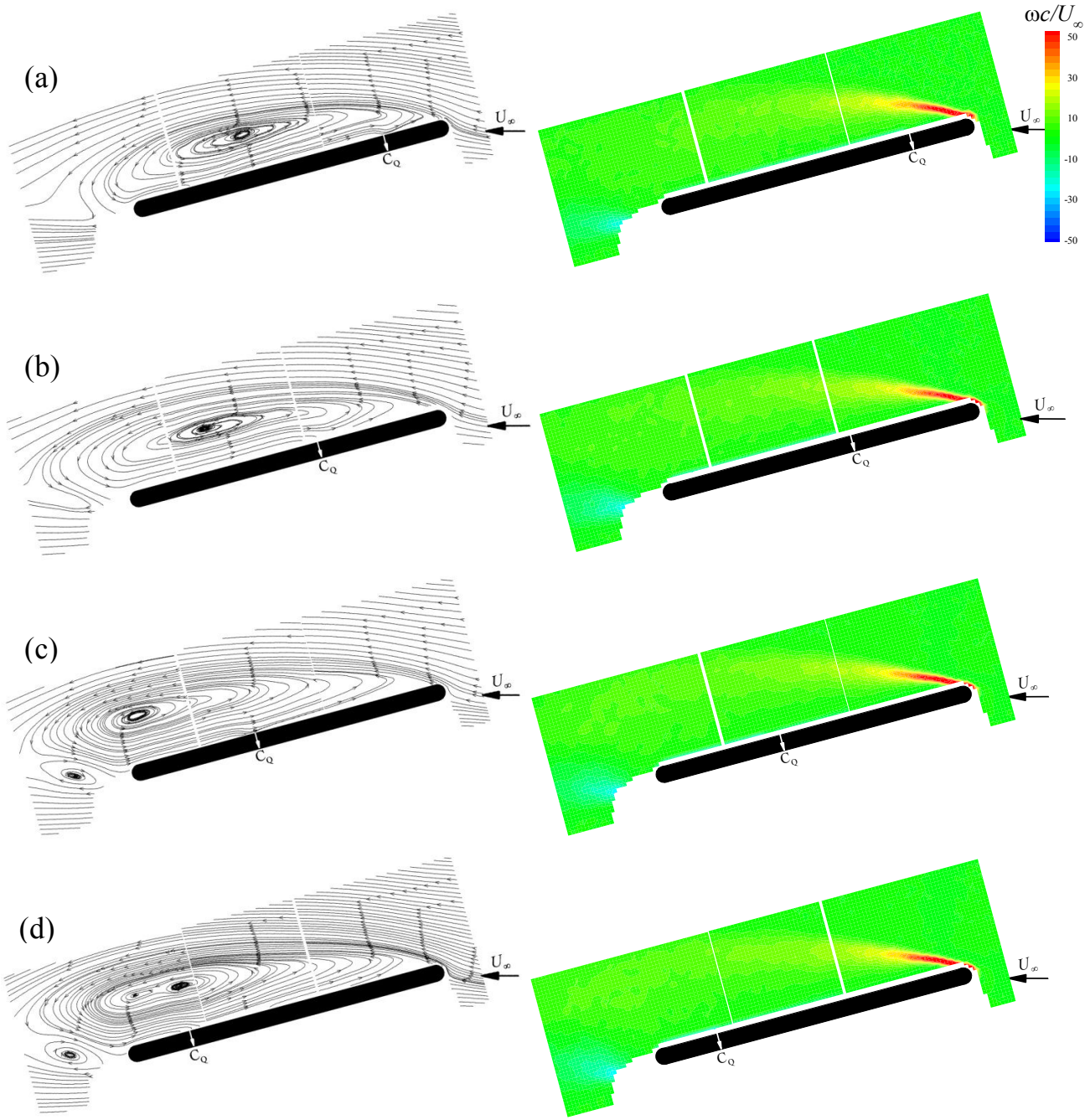

Figure 11. Streamline pattern (left column) and non-dimensional spanwise vorticity (right column) measured in a streamwise plane at midspan of the flat-plate airfoil at α = 15° with suction of C_Q = 0.0125 at (a) x_s/c=0.2, (b) x_s/c=0.4, (c) x_s/c=0.6, (d) x_s/c=0.8.

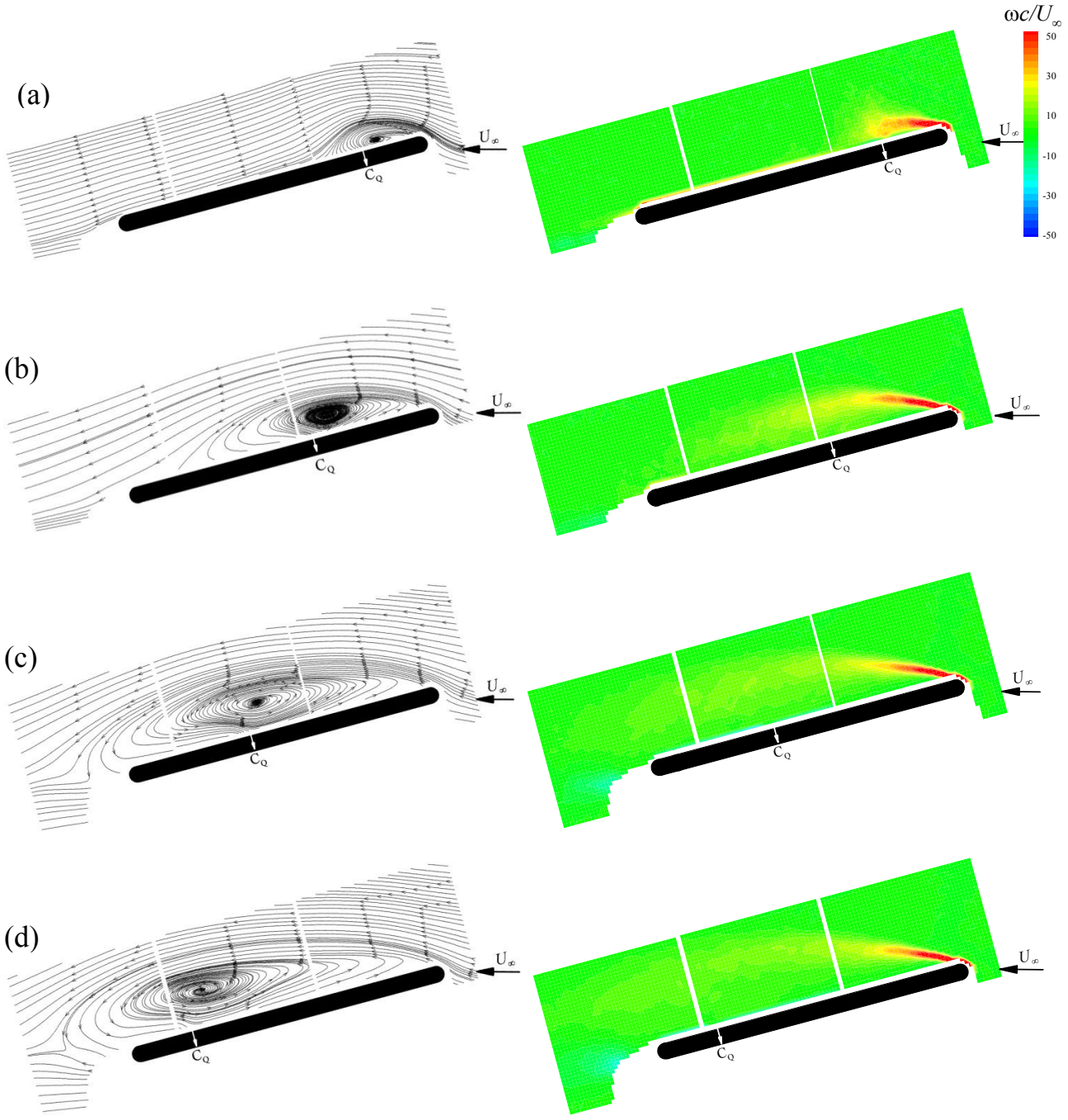

Figure 12. Streamline pattern (left column) and non-dimensional spanwise vorticity (right column) measured in a streamwise plane at midspan of the flat-plate airfoil at $\alpha = 15^{o}$ with suction of $C_Q = 0.0292$ at (a) x_s/c=0.2; (b) x_s/c=0.4; (c) x_s/c=0.6; (d) x_s/c=0.8.